

รายงานวิจัยฉบับสมบรูณ์

โครงการ
การใช้เทคนิคด้านวิศวกรรมขอบเกรนปรับปรุงคุณสมบัติ
บริเวณขอบเกรนของเหล็กกล้าไร้สนิม 304
Grain Boundary Engineering to Improve
Intergranular Properties of 304 Stainless Steel

โดย ผศ.ดร.วิศิษฐ ทวีปรังษีพร

วันที่ 30 พฤศจิกายน พ.ศ. 2543

สัญญาเลขที่ RSA/02/2540

รายงานวิจัยฉบับสมบรูณ์

โครงการ การใช้เทคนิคด้านวิศวกรรมขอบเกรนปรับปรุงคุณสมบัติ บริเวณขอบเกรนของเหล็กกล้าไร้สนิม 304 Grain Boundary Engineering to Improve Intergranular Properties of 304 Stainless Steel

ผศ. ดร. วิศิษฐ ทวีปรังษีพร ภาควิชานิวเคลียร์เทคโนโลยี คณะวิศวกรรมศาสตร์ จุฬาลงกรณ์มหาวิทยาลัย

สนับสนุนโดยสำนักงานกองทุนสนับสนุนการวิจัย

ACKNOWLEDGMENTS

The principal investigator gratefully acknowledge the financial support provided by the Thailand Research Fund under contract no. RSA 2/2540. Without this funding, not only that this research can never get started but also several students will never have the support needed to complete their research that they can be proud of.

Several faculty members and graduate students contribute significantly towards the completion of this work. Asst.Prof. Suvit Punnachaiya and Mr. Decho Thong-Aram (Lecturer) both in the dept of nuclear technology, Chulalongkorn University, were the key researchers in designing and construction of several unique facilities developed for this research. My former graduate students, Ms. Porrawan Swatewacharkul, Mr. Kullawat Talerngsuk, Ms. Piyaporn Sinsrok, and their peers were very helpful and I greatly appreciate their assistance. Thanks also to my lab manager, Mr. Somchai Baotong, and current graduate students, Mr. Kittisuk Kosolwanthana and Ms. Patrisa Pumpruek, for generating several important data for this research. Further, I personally appreciate all of the above-mentioned people for making the working atmosphere in the Nuclear Engineering Material Laboratory an enjoyable one. Finally, the donation of all stainless steel used in this research from ThaiNox Steels is much appreciated.

รหัสโครงการ : RSA/02/2540

ชื่อโครงการ: การใช้เทคนิคด้านวิศวกรรมขอบเกรนปรับปรุงคุณสมบัติบริเวณขอบเกรนของเหล็กกล้าไร้สนิม 304

ชื่อนักวิจัย : ผู้ช่วยศาสตราจารย์ ดร. วิศิษฐ ทวีปรังษีพร

ระยะเวลาโครงการ : 1 ธันวาคม 2540 ถึง 30 พฤศจิกายน 2543

งานวิจัยนี้มีจุดประสงค์เพื่อใช้เทคนิคด้านวิศวกรรมขอบเกรนปรับปรุงคุณสมบัติบริเวณ ขอบเกรนของเหล็กกล้าไร้สนิม 304 งานวิจัยได้แบ่งออกเป็น 3 ส่วน คือ 1.การพัฒนาเครื่องมือ และการทดลองที่จำเป็นต่องานวิจัย 2.การวิเคราะห์ลักษณะขอบเกรนด้วยเทคนิคด่างๆ 3.การ ประเมินคุณสมบัติการแตกตามขอบเกรนของวัสดุที่ผ่านกระบวนการทางวิศวกรรมขอบเกรน

เครื่องมือและอุปกรณ์หลายชนิดได้ถูกพัฒนาขึ้นเพื่อนำมาใช้ในงานวิจัยนี้โดยเฉพาะ อันได้แก่ เครื่องมือทดสอบการดึงด้วยอัตราเร็วการยืดต่ำได้ถูกพัฒนาขึ้นเพื่อทดสอบการดึงที่ อัตราเร็ว 5x10⁻⁵ มม./วินาที ขณะที่ชิ้นงานอยู่ในสารละลายเคมี ผลร่วมจากอัตราเร็วการยืดต่ำ และสิ่งแวดล้อมที่รุนแรงต่อการเกิดการกัดกร่อน จะมีประโยชน์ต่อการทดสอบความไหวตัวต่อ การเกิดการแตกตามขอบเกรนจากผลของความเค้น เตาอบที่สามารถควบคุมบรรยากาศได้ก็ถูก พัฒนาขึ้นเพื่อใช้ในกระบวนการให้ความร้อนในกาชต่างๆ นอกจากนั้นยังมีการพัฒนาเทคนิค การขัดและกัดผิวหน้าโดยวิธีทางเคมีไฟฟ้าเพื่อช่วยในการเตรียมชิ้นงาน ซึ่งจะนำไปตรวจสอบ ลักษณะโครงสร้างจุลภาคต่อไป และยังมีการใช้เทคนิคการกระเจิงกลับของอิเล็กตรอนในการ ตรวจจับอิเล็กตรอนที่กระเจิงออกจากผิวหน้าของชิ้นงานเพื่อบอกลักษณะของขอบเกรน การ วิเคราะห์นี้เป็นไปแบบอัตโนมัติและสามารถวิเคราะห์ในพื้นที่ 100 μm² ภายในเวลา 2-3 ชั่วโมง จากการจัดเรียงตัวของเกรนและความแตกต่างระหว่างมุมจะสามารถบอกถึงลักษณะการ กระจายของขอบเกรนในชิ้นงานได้

จากการทดสอบทางความร้อนเชิงกลแบบต่างๆ เราพบว่ากระบวนการที่เหมาะสมทำได้ โดยผ่านการให้ความเครียดร่วมกับความร้อนเท่านั้น ความสำเร็จที่เกิดขึ้นในขั้นดัน คือ การให้ ความเครียดวัสดุประมาณ 3-5% ตามด้วยการให้ความร้อนที่ 950°C เป็นเวลา 10 นาที 3 รอบ โดยจะมีขนาดของเกรน เท่ากับ 30 µm และพบว่าสัดส่วนของขอบเกรนจะเพิ่มขึ้นโดยเฉลี่ยจาก 35% เป็น 57% ซึ่งสัดส่วนที่เพิ่มขึ้นนี้จะสามารถลดการกัดกร่อนที่ขอบเกรนซึ่งได้ผ่านการเซนซิ ไทซ์แล้วที่ 650°C เป็นเวลา 2 ชั่วโมง ได้เป็นอย่างมาก จากการทดสอบด้วยกรดออกซาลิก

ในความพยายามที่จะลดขนาดของขอบเกรนและกระบวนการความร้อนเชิงกล 3 ขั้น ตอนข้างต้น จึงได้มีการพัฒนากระบวนการใหม่ขึ้นมา อันได้แก่ การทำให้เสถียรโดยความร้อนที่ 900°C เป็นเวลา 1 ชั่วโมงตามด้วยการรีดเย็น 3% และให้ความร้อนที่ 900°C เป็นเวลา 3 นาที จะได้เกรนที่มีขนาด 15 µm กระบวนการนี้ส่งผลให้วัสดุมีความทนต่อการแตกโดยผลของความ เค้นได้สูงมาก จากการทดสอบการดึงด้วยอัตราเร็วการยึดต่ำของชิ้นงานที่ผ่านการเซนซิไทซ์ ที่ 650°C เป็นเวลา 8 ชั่วโมง แสดงให้เห็นว่าวัสดุที่ผ่านกระบวนการการปรับปรุงขอบเกรนเพิ่ม ความสามารถในการยึดจากเพียง 5% เป็น 60% นั่นคือการปรับปรุงคุณสมบัติเชิงกลของวัสดุ มากกว่า 10 เท่า กระบวนการผลิตที่มีความทนต่อการแตกหักสูงขึ้นนี้กำลังเตรียมดำเนินการจด สิทธิบัตรและเดรียมตีพิมพ์ระดับนานาชาติหลังจากการยื่นจดสิทธิบัตรเสร็จสมบูรณ์

คำหลัก: วิศวกรรมขอบเกรน สัดส่วนของขอบเกรน กระบวนการทางความร้อนเชิงกล การกัดกร่อนตามขอบเกรน Project Code: RSA/02/2540

Project Title: Grain Boundary Engineering to Improve Intergranular Properties

of 304 Stainless Steels

Investigator: Asst.Prof.Dr. Visit Thaveeprungsriporn

E-mail Address: fntvtv@eng.chula.ac.th

Project Period: December 1, 1997 to November 30, 2000

The overall objective of this research program is to improve intergranular properties of 304 stainless steels via grain boundary engineering. The research program was separated into 3 phases: 1) Development of experimental infrastructure including specimen preparation capability, 2) Characterization and engineering of grain boundary; and 3) Evaluating intergranular properties of grain boundary engineered materials. This research intends to demonstrate that intergranular properties of 304 stainless steel can be significantly improved by the use of simple thermomechanical processing to realign the grain boundary structures into a lower energy state such that these grain boundaries are intrinsically resistant to corrosion.

Several unique facilities were developed for this research. The environmental slow strain rate tensile testing (SSRT) was developed to perform tensile testing at an extremely slow rate ($5x10^\circ$ mm/s or 0.18 mm/hr) while specimen is immersed in a recirculating chemical solution. The combined effect of slow strain rate and aggressive environment is beneficial in testing for its susceptibility to stress corrosion cracking. A controlled atmosphere furnace was developed for performing heat treatment in any chosen gaseous environment. Electropolishing and electroetching unit was also developed in-house for preparing specimen surface for microstructure characterization. Grain boundary characterization was performed using an electron back-scattering diffraction system. This unique technique captures Bragg diffracted back-scattered electrons from the specimen surface. An automatic diffraction pattern analysis was performed on-line allowing a 100 μ m area to be analyzed within a few hours. Information on grain orientation and misorientation were used to obtain how grain boundaries distributed in a given specimen.

Extensive investigation on different thermomechanical treatments reveal that practical processes could only be achieved via strain annealing – light deformation follow by short time heat treatment. Our initial success occurred via the use of iterative strain annealing consisting of 3 sequential low deformation (3-5%) followed by short heat treatment at 950°C for 10 min. The mean grain size of this process is 30 µm. It was found that the fraction of special boundary (coincidence-site-lattice, CSL) was increased from an average of 35% to 57%. This moderate increase in the CSL fraction was found to significantly reduce the attack at the grain boundary area from oxalic acid after sensitized the specimen at 650°C for 2 hr.

On further evaluation of strain annealing technique to reduce the grain size and the cycle time of 3 strain annealing steps, a new treatment was developed and the result was striking. This special treatment consists of one step thermal stabilization at 900°C for 1 hr followed by 1 step strain annealing employing 3% strain and heat treatment at 900°C for 3 min while keeping the mean grain size at 15 μm . This results in a significant improvement in stress corrosion cracking susceptibility. SSRT tests of specimens sensitized at 650°C for 8 hr indicated that grain boundary engineered specimens show an improvement in ductility from a mere 5% in as-received specimens to 60% - a more than 10 folds improvement. This current thermomechanical treatment is now being filed for patent and an international publication is being prepared upon the completion of patent filing process.

Keywords: grain boundary engineering, coincidence-site-lattice boundary, thermomechanical processing, intergranular stress corrosion cracking

Contents

	Page
Acknowledgments	
Abstract (Thai)	
Abstract (English)	
Contents	
List of tables	vii
List of figures	viii
Introduction	
Experiments	2
Results and discussion	
References	15
Summary of output	16
Appendix	
The effect of grain boundary character distribution on in tergranular	
corrosion of 304 stainless steel	18
Effect of interative strain annealing on grain boundary network of	
304 stainless steel	21

List of Tables

	Page
Table 1. Summary of the effect of iterative strain anneal on grain size	
and CSLB population	8
Table 2. Summary of SSRT tests in 0.5M Na ₂ S ₂ O ₃ – pH 4	

List of Figures

Page
Figure 1. Illustration of the effect of grain boundary structure
on intergranular corrosion in the weld-decay region
of 304 stainless steel [4]. a) Optical and b) SEM
micrographs of grain boundaries (GB1 is Σ5 CSL
boundary while GB2 and GB3 are random boundary)
Figure 2. Slow Strain Rate Tensile Test (SSRT)
Figure 3. High Temperature Furnace
Figure 4. Schematic illustration of an EBSD System5
Figure 5. The effect of CSLB fraction on intergranular corrosion
of specimens with (a) 36% CSLB fraction and (b) 54 %
CSLB fraction6
Figure 6. Shows the scanning electron micrographs of as-received.
(a) and (c) and grain boundary engineered samples (b) and
(d) before and after sensitization at 650°C for 8 hr, respectively.
All specimens were electroetched using oxalic acid6
Figure 7. The effect of iterative strain annealing on dihedral angle distribution10
Figure 8. Correlation between the CSLB fraction and the standard deviation
of dihedral angle distribution11
Figure 9. Correlation between the cumulative frequency of dihedral
angle distribution and grain boundary character distribution11
Figure 10. Shows the stress-strain curves of all specimens tested.
Non-sensitized AR (e), GBE (d) and Sensitized at 650°C/8 hr
GBE (c, f), AR (a, b)12
Figure 11. Shows cross sectional area of specimens after failure.
(a) non-sensitized as-received, (b) non-sensitized grain
boundary engineered, (c) sensitized grain boundary engineered,
and (d) sensitized as-received specimen
Figure 12. SEM micrographs of fractures. (a) non-sensitized as-received,
(b) non-sensitized grain boundary engineered, (c) sensitized
grain boundary engineered, and (d) sensitized as-received specimen 14
Figure 13. The dihedral angles distribution of GBE and As-received14

INTRODUCTION

Numerous failures of 304 stainless steels have occurred because of intergranular stress corrosion cracking (IGSCC). These happen in environments where the alloy should exhibit excellent corrosion resistance representing a tremendous economic loss and more importantly, pose safety concerns in the plants. This research focuses on improving IGSCC susceptibility of stainless steels via altering grain boundary intrinsic structure. Problems of IGSCC in austenitic stainless steels have long been recognized in industries and much effort has been done to minimize and prevent it from occurring. Thus far, this effort has led to an understanding of mechanisms which are responsible for IGSCC. Extensive research using electron microscopy indicates that the precipitation of chromium carbides at grain boundaries leading to grain boundary chromium depletion increases the IGSCC susceptibility in stainless steels. The phenomenon is known as sensitization.

Several literatures indicate that there exists a relationship between the occurrence of intergranular carbides and crystallographic nature of grain boundary. Butler and Burke [1] showed that severe chromium depletion profile is measured at high angle boundaries while ordered boundaries such as incoherent and coherent twin showed little or no chromium depletion. Carbides precipitation was also absent at coherent twin boundaries with limited precipitation takes place at incoherent twin boundaries which are consistent with the observed lack of chromium depletion. Limited precipitation takes place at incoherent twin boundaries and this causes a very narrow depleted region (< 50 nm), while the extensive precipitation of chromium-rich carbides which occurs at high-angle random boundaries leads to the widest chromium-depleted zones. In addition, earlier works on the related subject by Benett and Pickering [2] and Ortner and Randle [3] have also supported the importance of the grain boundary structure on the degree of sensitization in stainless steels. Figure 1 illustrates the effect of grain boundary structure on intergranular corrosion [4].

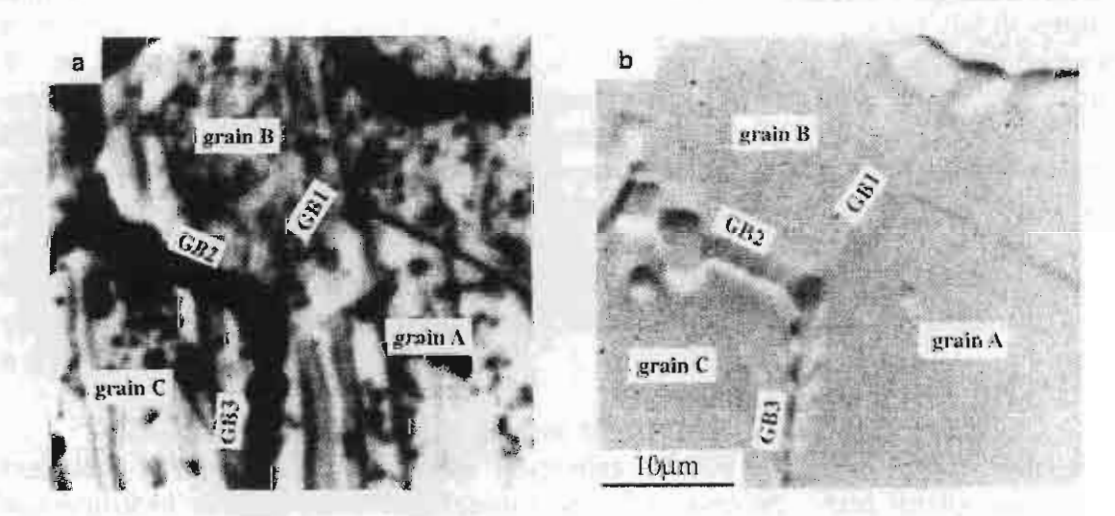


Figure 1. Illustration of the effect of grain boundary structure on intergranular corrosion in the weld-decay region of 304 stainless steel [4]. a) Optical and b) SEM micrographs of grain boundaries (GB1 is Σ 5 CSL boundary while GB2 and GB3 are random boundary)

These findings provide the crucial fact that not all grain boundaries possess identical properties and their structures could significantly influence intergranular properties. Since CSLBs are more resistant to intergranular carbide precipitation, thus chromium depletion, making these boundaries highly resistant to IGSCC while intergranular carbides prefer to precipitate on HABs causing these boundaries susceptible to IGSCC. As such, it thus sounds logical that the fraction of CSLBs presence in 304 stainless steels could influence the bulk sample resistance to IGSCC.

This research is thus aimed at addressing the effect of frequency and type of grain boundary distributed (grain boundary character distribution) on IGSCC of 304 stainless steels. It is envisaged that 304 stainless steels may be processed to be highly resistant to IGSCC by reducing the HAB population and increasing the population of CSLBs. This would result in a decrease of possible sites for intergranular carbides precipitate and thus sensitization. Not only the importance of grain boundary character distribution on IGSCC of stainless steels can be realized through systematic studies of this research, the approach to improve intergranular properties of stainless steels via grain boundary engineering may also lead to an innovative way of processing a new commercial heat of stainless steels which is highly resistance to IGSCC.

EXPERIMENTS

The first phase in this project involved the design and construction of experimental infrastructure needed to complete this research. There are mainly 3 principle instruments: 1) Slow strain rate tensile (SSRT) testing unit; 2) Controlled atmosphere high temperature furnace; and 3) Electron back-scattering diffraction (EBSD) system. The environmental slow strain rate tensile testing (SSRT) was developed to perform tensile testing at an extremely slow rate (5x10⁻⁵ mm/s or 0.18 mm/hr) while specimen is immersed in a re-circulating chemical solution. combined effect of slow strain rate and aggressive environment is beneficial in testing for its susceptibility to stress corrosion cracking. A controlled atmosphere furnace was developed for performing heat treatment in any chosen gaseous environment. Grain boundary characterization was performed using an EBSD system at Scientific and Technological Research Equipment Center (STREC), Chulalongkorn University. This unique technique captures Bragg diffracted back-scattered electrons from the specimen surface. An automatic diffraction pattern analysis was performed on-line allowing a 100 µm² area to be analyzed within a few hours. Information on grain orientation and misorientation were used to obtain how grain boundaries distributed in a given specimen.

The second phase of this project involved with the engineering of grain boundary to improve intergranular properties of 304 stainless steel. This was accomplished via the use of thermomechanical processing. And finally, the grain boundary engineered stainless steels were tested for their susceptibility to intergranular stress corrosion cracking via the use of SSRT in an aggressive environment.

1. Environmental Slow Strain Rate Tensile Test

The environmental slow strain rate tensile test is used to perform stress corrosion cracking test while specimen is immersed in a re-circulating chemical solution, Figure 2. The SSRT is designed to perform tensile or compressive test in hazardous environment at a very low extension rate (5x10⁻⁵ mm/s). The load frame is entirely made of carbon steels. The upper pull rod is threaded and fixed to the upper load frame while the lower pull rod is attached to a lead screw driven by a reduced gearbox with a ratio of 1:18,000 providing a very low extension rate. The gearbox is powered by a ¼ HP motor capable of adjusting speed from 0-30 rpm. An OMEGA linear variable differential transformer (LVDT) displacement transducer is employed for extension measurement with a resolution better than 2 µm/mV. A 1000 lb miniature load cell obtained from Transducer Technique is attached to the upper pull rod for measuring forced being applied onto the specimen. During testing, a specimen is situated inside a chemical cell made of plexi-glass with an inlet and an outlet connected to a chemical pump for chemical solution to be continuously re-circulated.

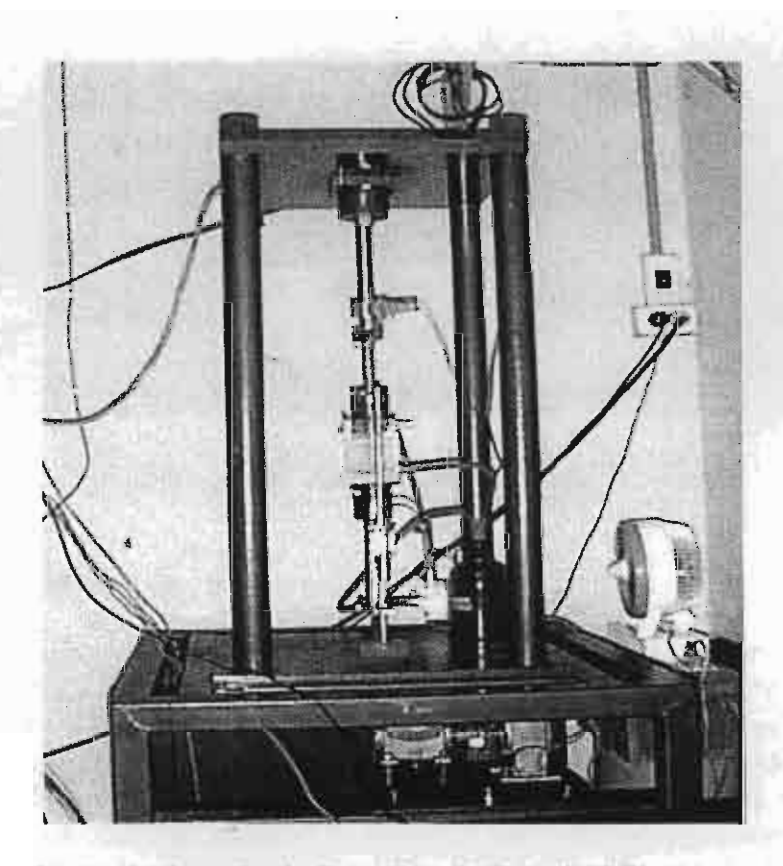


Figure 2. Slow Strain Rate Tensile Test (SSRT).

2. Controlled Atmosphere High Temperature Furnace

All heat treatments were performed in a Lindberg tube furnace under flowing nitrogen gas, Figure 3. This furnace is capable of operating at a temperature up to 1200°C. The furnace tube is made of quartz and the temperature controller CN9000A OMEGA is used to provide constant temperature. A type-K thermocouple extending through the quartz tube into the center of the hot zone provided temperature measurement near the samples. At the end of heat treatments, the sample was pushed out of the tube with a 310 stainless steel push rod and quenched in a water bath attached to the other end of the quartz tube.

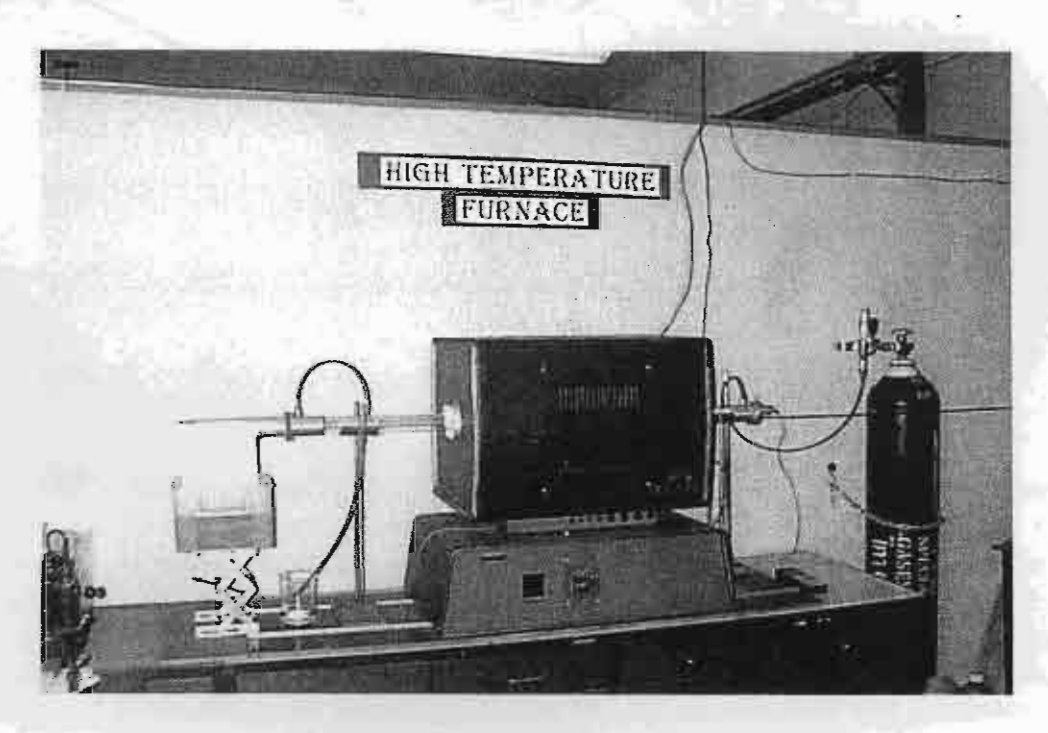


Figure 3. High Temperature Furnace.

3. Electron Back-Scattering Diffraction System

The crystallographic orientation of specimen was characterized using an automatic EBSD system under the trade name of OPAL in JEOL 5800LV scanning electron microscope. The EBSD system consists of a highly tilted specimen stage, a low-light TV camera interfaced to phosphor screen and a dedicated computer. As an electron beam is focused onto the specimen mounted on a highly tilted specimen, Bragg diffracted back-scattered electron is projected onto the phosphor screen where the low-light TV camera is used to view the diffraction pattern through the back of the screen, Figure 4. The real time picture of the pattern is then viewed on a monitor and analyzed using a computer driven cursor and dedicated software.

EBSD System

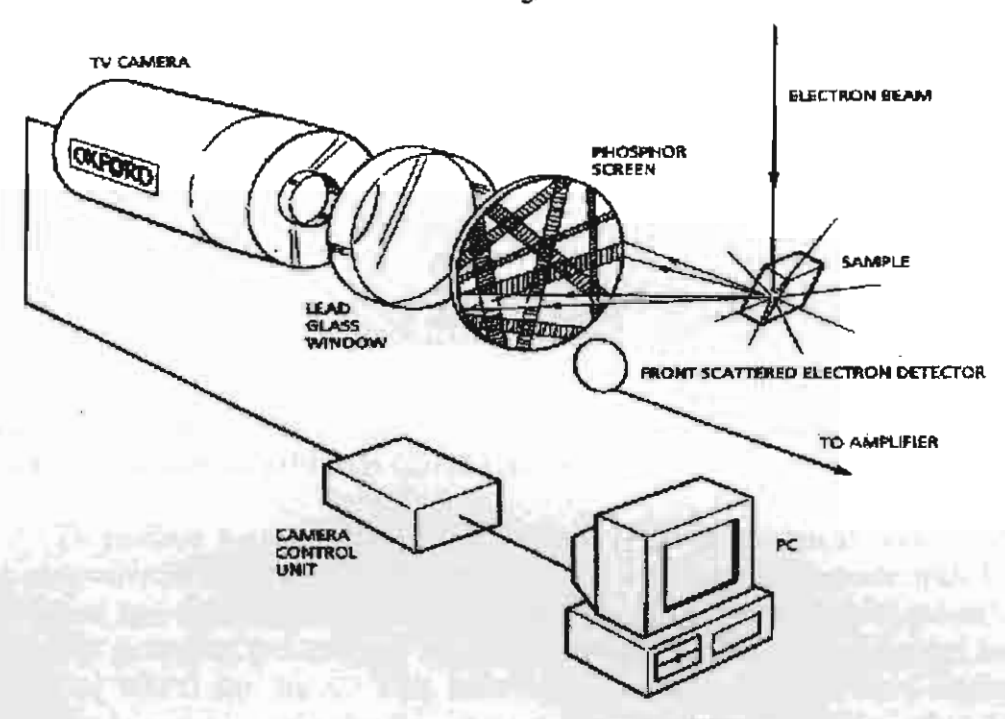


Figure 4. Schematic illustration of an EBSD System.

The equipment is located at the Scientific and Technological Research Equipment Center (STREC). The information from EBSD allows us to get an insight into orientation distribution and grain boundary character distribution of each specimen condition. The CSLB classification was based on Brandon's criterion (5) and only Σ values up to 29 are considered. Dihedral angles were measured directly from scanning electron micrographs taken at a minimum magnification of 750x. For each sample, at least 200 grains were crystallographically characterized and more than 70 triple junctions (210 grain boundaries) were quantified for their dihedral angles. It should be noted that triple junctions containing coherent twin boundaries were excluded from the dihedral angle measurement.

4. Grain Boundary Engineering of 304 S-Steel

As-received 304 stainless steel rods (Fe-18.5Cr-9.2Ni-1.07Mn-0.036C) were first sectioned into pieces of 2 inches long, and then solutionized at 1050°C for 2 hr. Specimens were then forged 30%, and recrystallized at 800°C for 0.5 hr, 850°C for 2 hr, and 950°C for 4 hr to produce different grain sizes. Specimens further received 3% in compression and annealed at 950°C for 10 min. A total of 3 sequential strain-annealing steps were employed. This heat treatment step results in a grain size of about 30-35 μ m. Figure 5 shows the micrographs of specimens with different grain boundary character distribution.

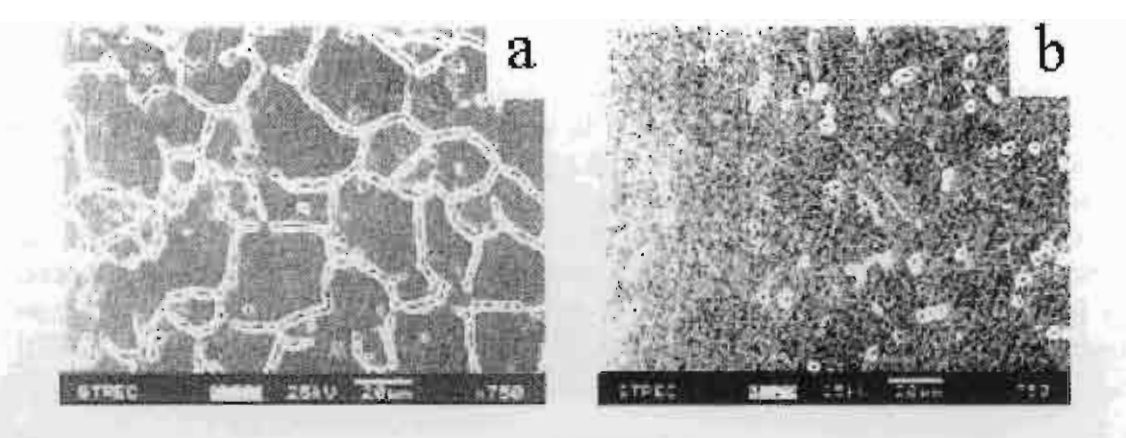


Figure 5 The effect of CSLB fraction on intergranular corrosion of specimens with (a) 36% CSLB fraction and (b) 54% CSLB fraction.

To produce a smaller grain size material, another treatment was developed. The as-received ThaiNox D189 (Fe-18.2Cr-9.0Ni-1.7Mn-0.044C) grade with 1.2 mm thick sheet was first stabilized at 900°C for 1 hr. After thermal stabilization, a one step strain annealing process was applied consisting of 3% strain followed by heat treating at 900°C for 3min. This heat treatment did not result in a statistically significant increase in grain size from the original as-received condition of 12-15 μm . Figure 6 shows the micrographs of samples of as-received and grain boundary engineered conditions.

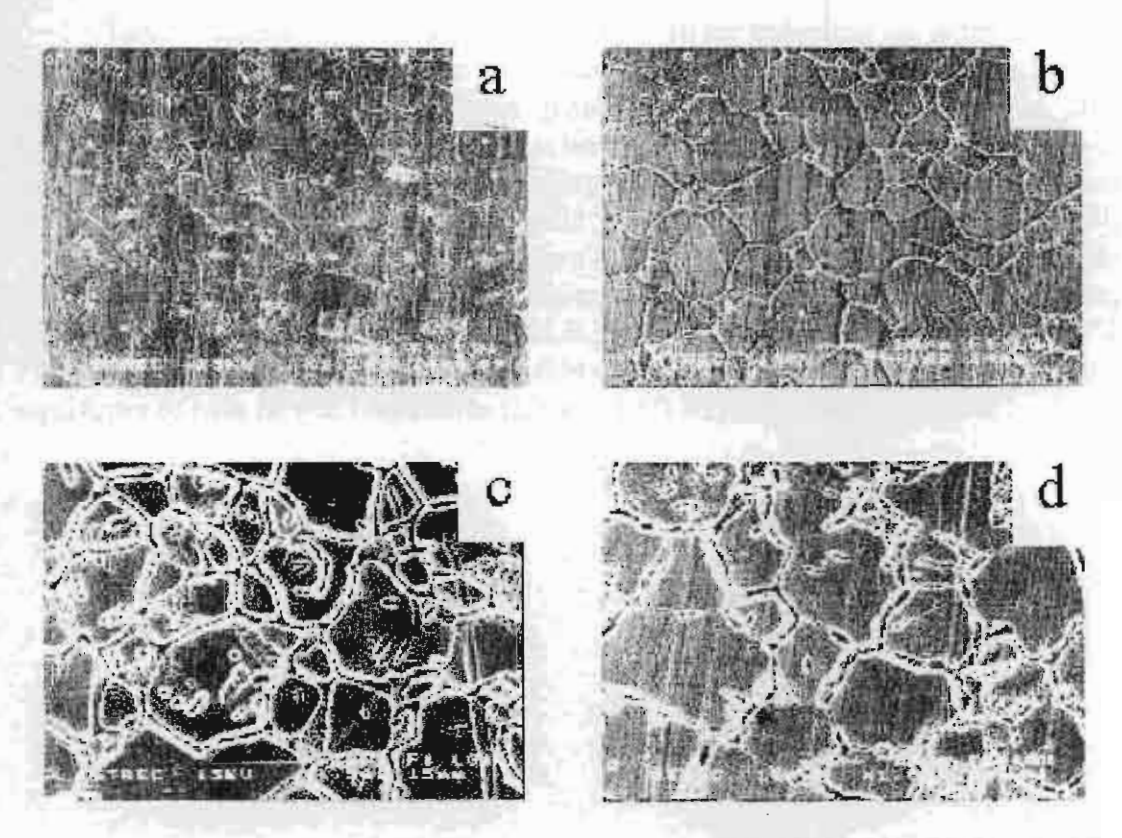


Figure 6 shows the scanning electron micrographs of as-received (a) and (c) and grain boundary engineered samples (b) and (d) before and after sensitization at 650°C for 8 hr, respectively. All specimens were electroetched using oxalic acid.

5. Stress Corrosion Cracking Test

Tensile specimens were machined from a 1.2mm thick sheet with a gagelength of 35 mm and 6mm in width. A solution of 0.5M Na₂S₂O₃.H₂O (Sodium thiosulfate pentahydrate) adjusted to a pH of 4 using a few drops of HCl was used to provide an aggressive environment. All specimens were tested in the thiosulfate solution at ambient temperature using an initial strain rate of 1.6x10⁻⁶ per second. Specimens were tested to failure and the stress-vs-strain curves were recorded. Some specimens were also aged at 650°C for 8 hr prior to testing to induce their susceptibility to IGSCC. After the test, fracture surfaces were examined in a scanning electron microscope (SEM) to reveal the nature of cracking.

RESULTS AND DISCUSSION

The results and discussion section is separated into 2 parts. The first part discusses the physical consequence of thermomechanical processing on grain boundary network. The other section presents the results from SSRT test comparing the IGSCC susceptibility of as-received and grain boundary engineered 304 stainless steels.

1. Effect of Thermomechanical Processing on Grain Boundary Network

Table 1 summarizes the effect of iterative strain annealing on grain sizes and CSLB distribution. Following the first strain-annealing step, the thermomechanical treatment had resulted in some grain growth in specimens recrystallized at 800° C/0.5hr and 850°C/2hr. However, almost no change in mean grain size was observed following the 2^{nd} and 3^{rd} strain annealing steps. The entire thermomechanical processes did not affect the mean grain size of specimens that were initially recrystallized at 950°C/4hr. Although there is no clear systematic pattern of how the CSLB distribution altered with each strain-annealing step, the third heat-treating step resulted in an overall increase in the CSLB fraction reaching the maximum of 57%. Further, nearly all of the CSLB fractions are Σ 3 boundaries and no statistical significant of twin related boundaries (Σ 9 and Σ 27) were observed.

Table 1. Summary of the effect of iterative strain annealing on grain size and CSLB

population.

рорининон.					 	<u>-</u>
Recrystallized Temperature and Time	Initial Grain Size (µm)	Initial CSLB Percent	Strain Annealed 3% compression + 950°C/10min	Mean Grain Size (µm)	CSLB Percent	Σ3 Percent
			1 st	25	32	24
800°C/0.5 hr	800°C/0.5 hr 14	36	2 nd	29	47	35
300 C/0.5 III			3 ^{rđ}	31	49	40
			1 st	31	47	41
850°C/2hr	24	34	2 nd	32	33	23
830 C/2III 24	54	3 rd	30	57	50	
			1 st	28	43	36
950°C/4hr	30	38	2 nd	31	42	31
930 C/4III	30	50	3 rd	28	47	42

Lin et al. (6) showed that at high $\Sigma 3$ densities (>40%), geometric contributions strongly influence the final $\Sigma 3^n$ distribution. The twin-limited microstructure (TLM) model first proposed by Palumbo et al. (7) suggests that the maximum theoretical limit of 67% $\Sigma 3$ should likely result in 100% CSL distribution. The absence of twin-related boundaries, $\Sigma 9$ and $\Sigma 27$, even with a $\Sigma 3$ fraction up to 50% did not support the TLM model. The $\Sigma 3$ regeneration model recently proposed by Randle (8) is more applicable to explain how the iterative strain annealing process only enhance the $\Sigma 3$ boundary fraction observed in this study. The model shows how interface interactions in a twinned material generate $\Sigma 3$ boundaries without promoting the $\Sigma 3^n$ boundaries. Further, the strain annealing treatments had resulted in very little change in mean grain size, and thus, the $\Sigma 3$ regeneration model which is based on the mobility and dislocation absorption mechanism rather than the Fullman-Fisher twin formation model via grain growth is more relevant.

A moderate increase in the CSLB distribution does not translate directly into an expected moderate improvement in properties. It has been shown that only a moderate increase in the CSLB fraction in high purity nickel-base alloy via iterative strain annealing can improve creep and cracking properties remarkably (9). It was proposed that the significant improvement on the observed creep behavior is associated with different grain boundary types conjoined at a triple junction. It is not an individual specialness of each CSLB that is important, but rather how it is distributed and influenced the entire grain boundary network connected through the triple junctions.

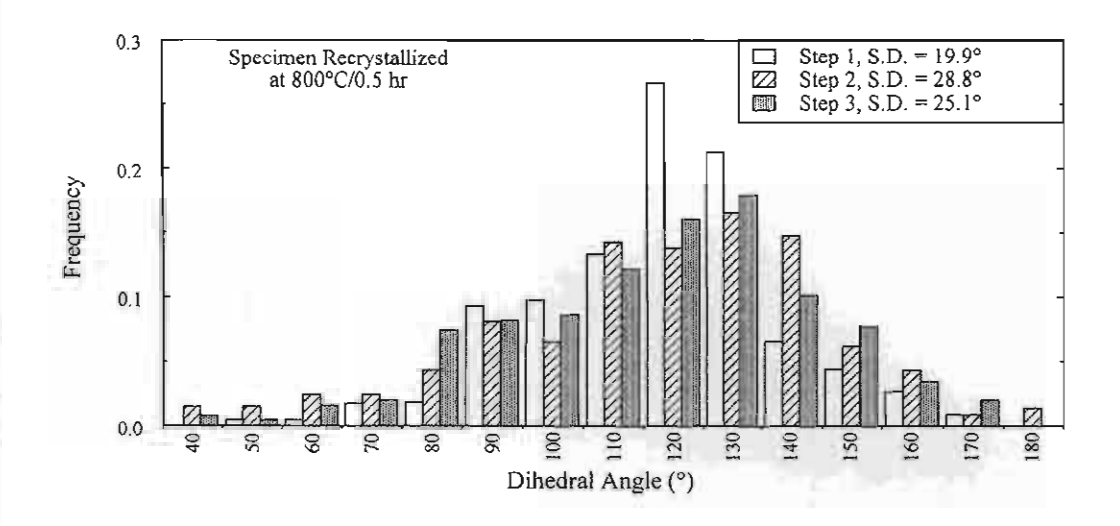
It is also well known that the specific free energies of grain boundaries meeting at a triple junction can be compared by measuring the equilibrium dihedral angles to the three grain boundaries (10,11). The dihedral angle is related to the grain boundary energy by the expression (12):

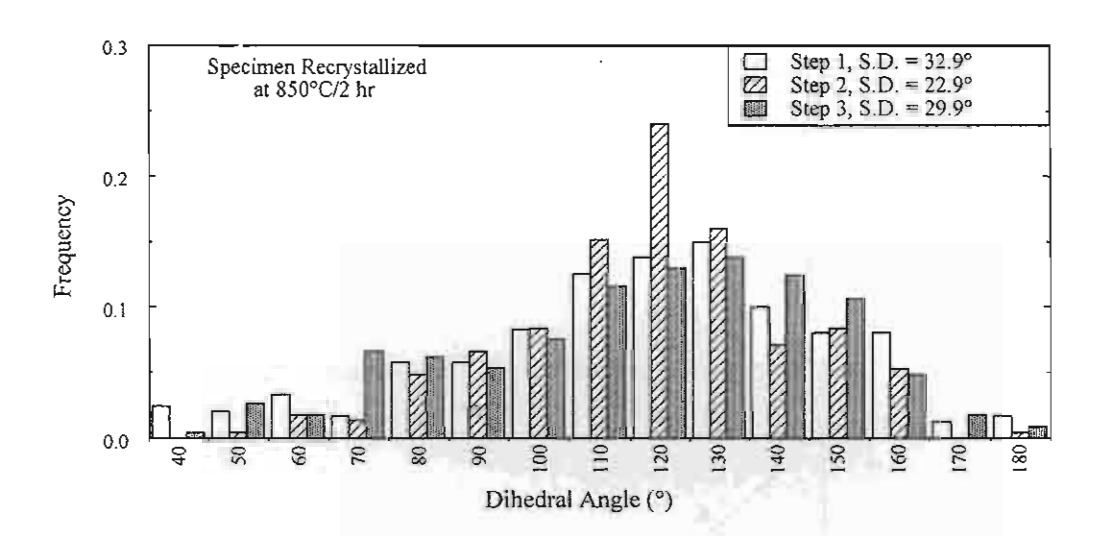
$$\gamma_a / \sin \alpha = \gamma_b / \sin \beta = \gamma_c / \sin \delta$$
; [1]

Where γ_a , γ_b , and γ_c are the grain boundary energies joined at a triple junction, and α , β and δ are the respective interfacial angles. Hence, the dihedral angle can be used as a measure of the grain boundary energy (13). Since the dihedral angle is related to the grain boundary network through surfaces connected along triple junctions, the measurement of dihedral angle distribution was adopted to explore a link between the CSLB distribution and its influence on the grain boundary network. Figure 7 summarizes the distribution of dihedral angles following each thermomechanical treatment. It can be seen that the distributions are very distinctive with some showing sharper distribution around 120° than others. It is also worth noting that despite very little change in the mean grain size there are substantial differences in dihedral angle distributions indicating significant grain boundary activities during each strain annealing step.

To statistically describe the dihedral angle distribution, the standard deviation (S.D.) which signifies the shape of the distribution was calculated and plotted with the CSLB distribution, Figure 8. It is clear that a fairly good linear correlation between the CSLB fraction and the standard deviation of the grain boundary dihedral angle distribution was observed. Higher CSLB fraction specimens possess a flatter distribution of dihedral angles while sharper distribution around 120° is observed in specimens with lower CSLB fraction. From eq.[1], if all three boundaries meeting at a triple junction are of equal in energies, a uniform 120° distribution is expected. Hence, various dihedral angle distributions of thermomechanically treated specimens indicate different proportions of energies presence in the system. In an attempt to quantifiably describe the dihedral angle distribution, the cumulative frequency of dihedral angles (CFDA) around the mean value of 120° was investigated. The CFDA parameter is introduced as a first approximation to describe grain boundary fraction within specific group of angles, and thus energies. Figure 9 shows the plot of the CFDA between 120°+/-10° and 120°+/-20° and grain boundary type fraction. It is interesting to see that the CFDA between 120°+/-10° accounts for nearly 40% in lower CSLB fraction. The CFDA monotonically decreases with decreasing high angle boundary (HAB) fraction or increasing CSLB fraction. The specimen with 57% CSLB fraction has a CFDA between 120°+/-10° of only 24%. The most striking result is the observed correlation between the HAB fraction and the CFDA between 120°+/-20°. The CFDA can be translated almost directly into the HAB fraction. This result clearly demonstrates that there is an intimate link between grain boundary type and its network.

As such, it is suggested here that the dihedral angle distribution can be used to provide information related to the grain boundary network, and thus the properties of polycrystals. Although it appears that the CSLB distribution is closely related to the dihedral angle distribution, the result may not be generalized. Since most of the CSLBs observed in this study are of $\Sigma 3$ type, these boundaries are likely to include a high proportion of tilt or twist boundary planes, and thus a lower energy configuration (13).





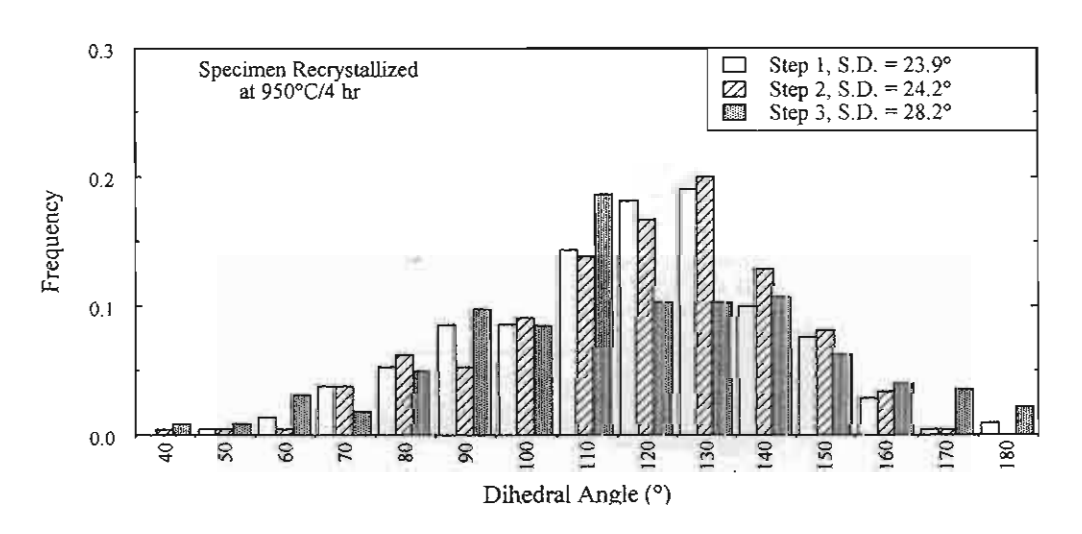


Figure 7. The effect of iterative strain annealing on dihedral angle distribution.

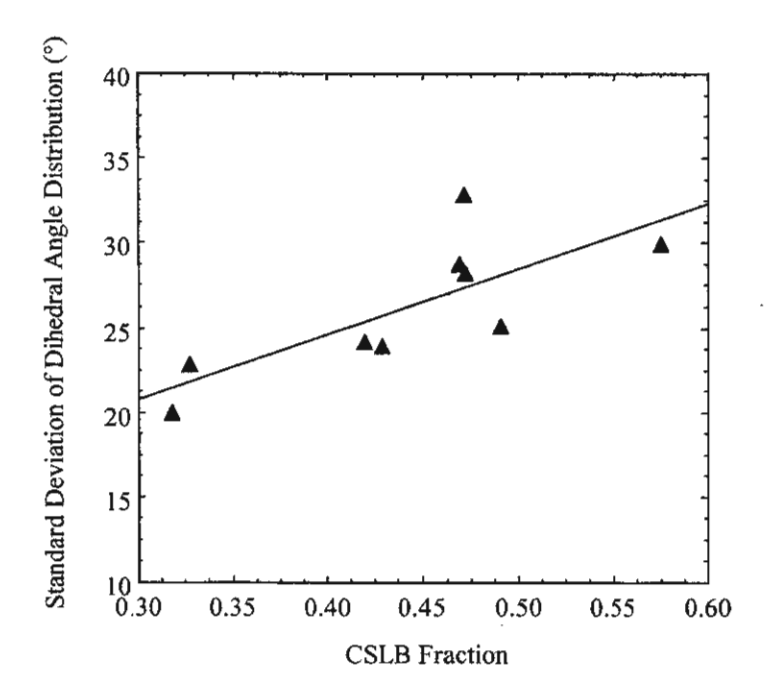


Figure 8. Correlation between the CSLB fraction and the standard deviation of dihedral angle distribution.

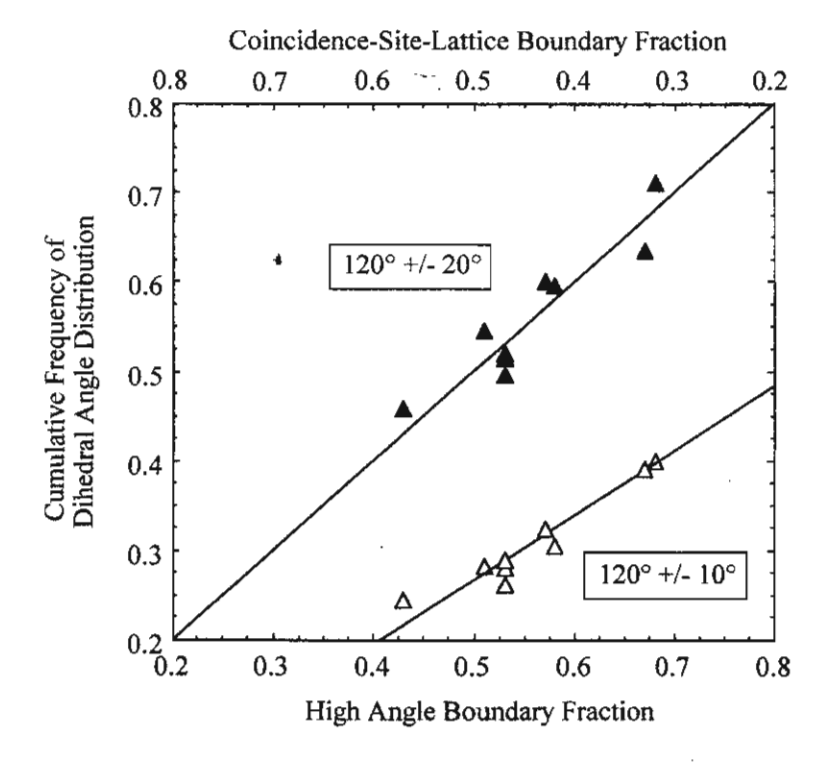


Figure 9. Correlation between the cumulative frequency of dihedral angle distribution and grain boundary character distribution.

6. Effect of Grain Boundary Network on IGSCC of 304 Stainless Steels

Figure 10 shows the stress-strain curves of all specimens tested. Two conditions of both as-received (AR) and grain boundary engineered (GBE) specimens were evaluated: non-sensitized and sensitized at 650°C for 8 hr. The non-sensitized condition of both AR and GBE specimens tested in sodium thiosulfate solution did not exhibit any susceptibility to IGSCC. Both specimens show good ductility up to nearly 70% strain. On testing the sensitized condition of both AR and GBE specimens, the result was strikingly different. The sensitized AR specimens exhibit extreme brittle failure with less than 5% strain at failure reaching the maximum tensile strength of less than 350 MPa. On the contrary, the sensitized GBE specimens demonstrate excellent ductility up to 60% strain at failure and a maximum tensile strength of similar to non-sensitized condition of approximately 700 MPa. Investigation of fracture surface also confirms the dimple-like structure characteristic of ductile failure mode. Table 2 summarizes the SSRT test results.

Engineering Stress vs Engineering Strain

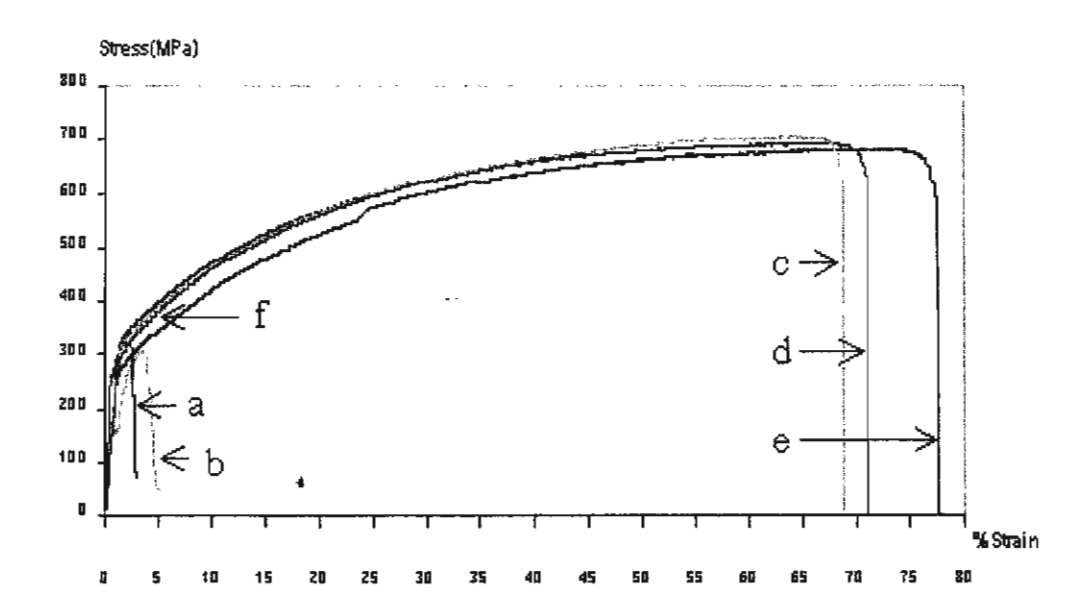


Figure 10. Shows the stress-strain curves of all specimens tested. Non-Sensitized AR (e), GBE (d) and Sensitized at 650 °C/8hr GBE (c, f), AR (a, b)

Figure 11 shows cross sectional area of specimens after failure. It can be clearly seen that except the sensitized AR specimen all specimens show a classical necking feature near the fracture surface. The nature of cracking was later confirmed by investigating high magnification scanning electron micrographs of fracture surfaces, Figure 12. The dimple structures in (a), (b), and (c) specimens indicate ductile failure mode via microvoid coalescence. The sensitized AR specimen however shows faceted-like structure on the fracture surface indicating complete intergranular cracking in this specimen.

Table 2 Summary of SSRT tests in 0.5M Na₂S₂O₃ - pH 4

Specimen Condition	Specimen Type	Yield Stress (MPa)	Max Tensile Strength (MPa)	Strain at Failure (%)	Fracture Mode
Non- Sensitized	As-received	260	675	70	Ductile
JA.	GBE	310	694	65	Ductile
Sensitized at	As-received	235 265	304 346	4.7	Brittle Brittle
650°C/8hr	GBE	280 290	704 672*	62 42*	Ductile *(experiment interrupted)

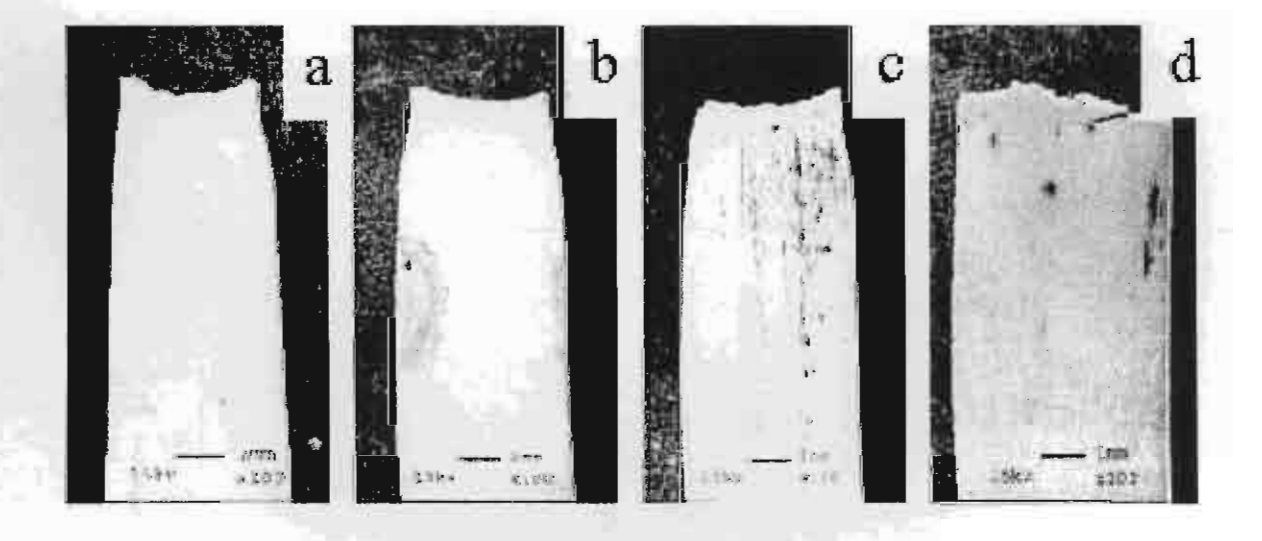


Figure 11. shows cross sectional area of specimens after failure. (a) non-sensitized asreceived, (b) non-sensitized grain boundary engineered, (c) sensitized grain boundary engineered, and (d) sensitized as-received specimen.

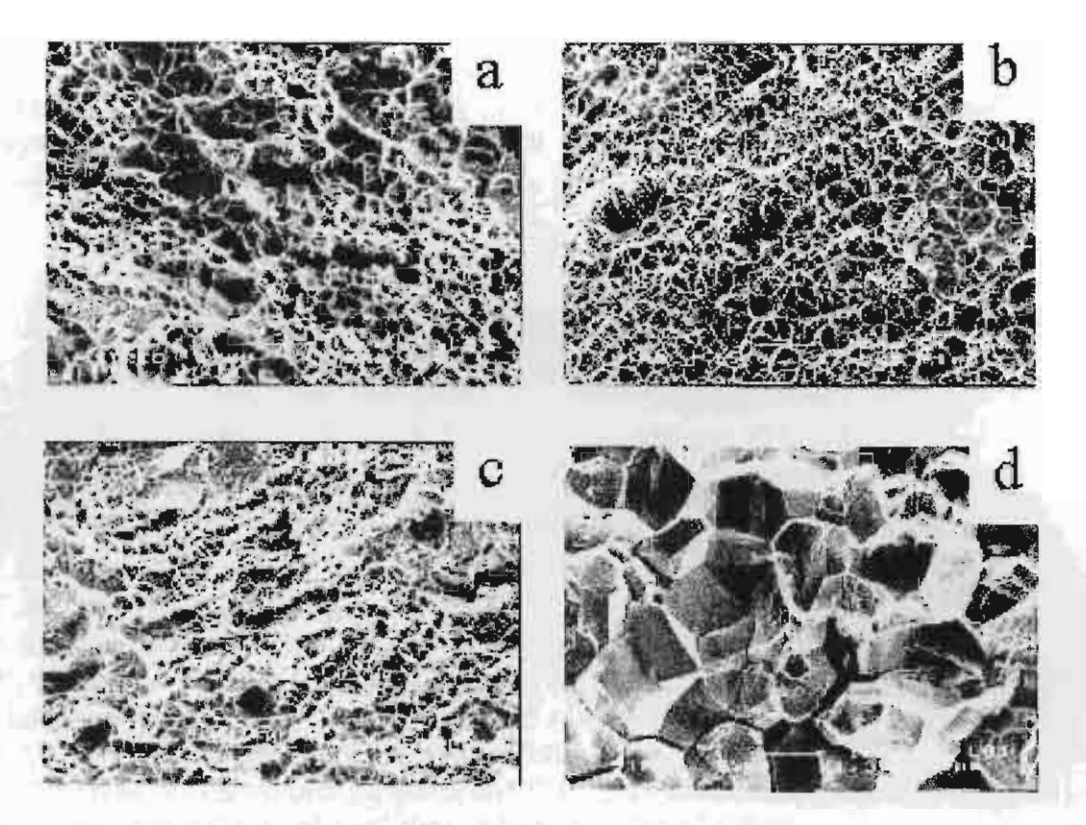


Figure 12. SEM micrographs of fracture surfaces. (a) non-sensitized as-received, (b) non-sensitized grain boundary engineered, (c) sensitized grain boundary engineered, and (d) sensitized as-received specimen.

Upon the investigation of grain boundary network by measuring the dihedral angle distribution, the GBE specimens show a flatter distribution of dihedral angles while sharper distribution around 120° is observed in AR specimens, Figure 13.

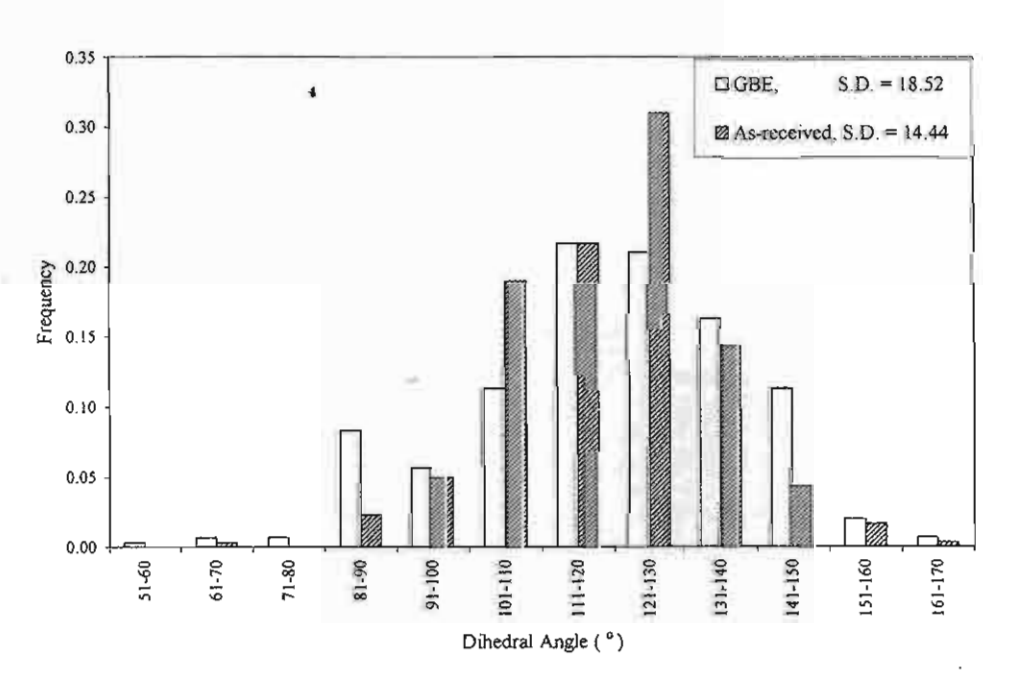


Figure 13. The dihedral angles distribution of GBE and As-received.

Following our previous discussion on grain boundary network, it can be concluded that various dihedral angle distributions of specimens indicate different proportions of energies presence in the system. The results clearly show that significant improvement on intergranular properties of 304 stainless steels can be achieved via a simple thermomechanical processing.

REFERENCES

- 1. E.P. Butler and M.G. Burke, Acta Metall., 3, 1986, pp. 557-570.
- 2. B.W. Bennett and H.W. Pickering, Metall. Trans. A, 18, 1987, pp. 1117-1124.
- 3. S.R. Ortner and V. Randle, Scripta Metall., 23, 1989, pp. 1903-1908.
- 4. H. Kokawa, M. Shimada, and Y. Sato, JOM, July, 52, (2000).
- 5. D.G. Brandon, Acta Metall., 14, 1966, pp. 1479.
- 6. P. Lin, G. Palumbo, and K.T. Aust, Scripta Mater. 36, 10, 1145 (1997).
- 7. G. Palumbo, K.T. Aust, U. Erb, P.J. King, A.M. Brennenstuhl, and P.C. Lichtenberger, Phys. Stat. Sol. (a) 131, 425 (1992).
- 8. V. Randle, Acta Mater. 47, 15, 4187 (1999).
- 9. G.S. Was, V. Thaveeprungsriporn, and D.C. Crawford, JOM, February, 44 (1998).
- 10. H. Gleiter and B. Chalmers, Prog. Mater. Sci. 16, 13 (1972).
- 11. L.E. Murr, Interfacial Phenomena in Metals and Alloys, Addison-Wesley, (1975).
- 12. C. Herring, in Physics of Powder Metallurgy, W. Kingston ed., McGraw-Hill, NY, (1951).
- 13. A. Morawiec, Scripta Mater. 41, 1, 13 (1999).
- 14. V. Randle, Mater. Sci. Technol. 7, 985 (1991).

SUMMARY OF OUTPUT

International Publication

• V. Thaveeprungsriporn, P. Sinsrok, and D. Thong-Aram, "<u>Effect of Iterative Strain Annealing on Grain Boundary Network of 304 Stainless Steel</u>", Scripta Materialia, accepted for publication August 2000, in press.

Master Degree Thesis

- Ms. Piyaporn Sinsrok, "Effects of Recrystallization and Grain Growth on the Formation of Annealing Twin in the 304 Stainless Steel", Master Degree Thesis in Dept of Nuclear Technology, Chulalongkorn University, ISBN 974-334-963-4, completed May, 2000.
- Mr. Kittisuk Kosolwanthana, "<u>Effect of Thermomechanical Processing on Stress Corrosion Cracking Susceptibility of 304 Stainless Steels</u>", Research Proposal Approved April 2000. Expected Graduation Date May 2001.
- Ms. Patrisa Pumpruek, "Sensitization of Thermomechanically Processed 304
 <u>Stainless Steel</u>, Research Proposal Approved April 2000. Expected Graduation
 Date August 2001.

National Conference and Seminar

- V. Thaveeprungsriporn, P. Sinsrok, and D. Thong-Aram, "The Effect of Grain Boundary Character Distribution on Intergranular Corrosion of 304 Stainless Steel", The First Thailand Materials Science and Technology Conference, organized by MTEC, July 2000.
- Special Seminar on <u>Materials Microanalysis Using Energy Dispersive X-ray Spectroscopy and Electron Back-Scattering Diffraction System</u>, Scientific and Technological Research Equipment Center, Chulalongkorn University, October 27, 2000.

In-Progress Output

- Preparing necessary documents to file for patent on grain boundary engineering of 304 stainless steel.
- Preparing an article to be submitted to **Scripta Materialia** entitled "<u>Effect of Grain Boundary Network on Intergranular Stress Corrosion Cracking of 304 Stainless Steel</u>", December 2000 (expected).

APPENDIX

Presented: The First Thailand Materials Science and Technology Conference, organized by MTEC, July 2000.

THE EFFECT OF GRAIN BOUNDARY CHARACTER DISTRIBUTION ON INTERGRANULAR CORROSION OF 304 STAINLESS STEEL

<u>Visit Thaveeprungsriporn</u>, Piyaporn Sinsrok, and Decho Thong-Aram Department of Nuclear Technology, Faculty of Engineering, Chulalongkorn University, Bangkok, Thailand, 10330

INTRODUCTION

Problems of intergranular corrosion (IGC) in austenitic stainless steels have long been recognized in industries, and much effort has been done to minimize and prevent it from occurring. Thus far, this effort has led to an established understanding of microstructure responsible for the degradation of intergranular properties in stainless steels. Extensive research using electron microscopy indicates that the precipitation of chromium carbides at grain boundaries leading to grain boundary chromium depletion increases the intergranular corrosion susceptibility in stainless steels. The phenomenon is known as sensitization. Perhaps one of the most well known examples of sensitization of austenitic stainless steels occurs as a result of welding. The thermal transient occurred during welding provides a temperature range suitable for chromium carbides to precipitate at grain boundaries.

A study on the relationship between the occurrence of intergranular carbides and crystallographic nature of grain boundary revealed that during sensitization the distribution of carbides at grain boundaries was not uniform [1]. It was found that boundaries which are more orderly structured (coincidence-site-lattice boundaries, CSLBs) were less susceptible to carbides precipitation while randomly oriented grain boundary structure (high angle boundaries, HABs) were heavily decorated with chromium carbides. This finding provides the crucial fact that not all grain boundaries possess identical properties and their structures could significantly influence intergranular properties. Since CSLBs are more resistant to intergranular carbide precipitation, thus chromium depletion, making these boundaries highly resistant to IGC while intergranular carbides prefer to precipitate on HABs causing these boundaries to be susceptible to IGC. As such, it thus sounds logical that the fraction of CSLBs presence in 304 stainless steels could influence the bulk sample resistance to IGC.

Interests in controlling grain boundary structure to achieve the desirable bulk properties in polycrystals have resulted in a search to find the processing parameters to enhance the frequency of CSLBs. Several reports describe the optimization of the CSLBs in high purity alloys through thermomechanical processing which relies on combinations of strain and annealing [2-4]. In this research, an iterative strain annealing processing has been developed to promote the population of CSLBs in commercial grade 304 stainless steel. The process involves three stages of low level of deformation followed by a short time heat treatment. Specimens with varying CSLB fraction were then sensitized and tested for their susceptibility to intergranular corrosion.

EXPERIMENTAL PROCEDURES

An as received 304 stainless steel rod was first solutionized at 1000°C for 1 hr. Specimens were then received 30% reduction in thickness and recrystallized at 800°C , 850°C , and 950°C for 30 min, 120 min and 240 min to produce different grain sizes, respectively. For each grain sizes, specimens were then received 3% reduction in thickness and annealed at 950°C for 10 min. A total of 3 sequential strain annealing steps were employed. After each step, specimens were characterized for their CSLB distribution using automatic electron back-scattering diffraction system. At least 150 grains were crystallographically characterized. Grain boundaries were characterized by the Σ number where Σ refers to the reciprocal density of coincident lattice points. The higher the Σ number, the grain boundary structure becomes less ordered. To investigate their susceptibility to intergranular corrosion, all thermomechanically treated specimens were sensitized at 650°C for 2 hr and electroetched in a solution of 10% oxalic acid. This solution attacks chromium-depleted boundaries and thus, indicates their susceptibility to intergranular corrosion.

RESULTS AND DISCUSSION

Table 1 summarizes the effect of iterative strain annealing on grain sizes and CSLB distribution. It was found that after 3 iterative strain annealing no significant grain growth was observed. The grain sizes were in the range between 24-32 μ m. The CSLB distribution also was not changed drastically. It is clear that the first 2 steps did not promote the CSL distribution which were ranging between 27% to 40%. The third heat treating step resulted in a moderate increase in the CSLB fraction reaching the maximum of 54% CSLB fraction. Most of the CSLB fraction is of Σ 3 boundaries and no statistical significant of twin related boundaries (Σ 9, and Σ 27) are observed. Figure 1 shows the comparison in CSLB distribution of specimens with 36% and 54% CSLB distribution. It can be seen that the only increase in the CSLB distribution occurs as a result of an increase in Σ 3 boundary. Lin et al. [5] showed that at high Σ 3 densities (>40%), geometric contributions strongly influence the final Σ 3 distribution, and the maximum theoretical limit of 67% Σ 3 should likely result in 100% CSL distribution. The absence of twin related boundaries, Σ 3ⁿ (Σ 3, Σ 9, and Σ 27), in this material may be a result of the level of impurities presence. It was pointed out that increasing impurity content result in diminished energy differences between CSLB and non-CSLB related interfaces due to selective impurity segregation [6].

Figure 2 shows the effect of CSLB fraction on the degree of sensitization. The specimen with 36% CSLB fraction was heavily attacked after sensitization while the specimen with 54% CSLB fraction shows very little corroded area after oxalic etched. This is in agreement with other researchers that only a moderate increase in the CSLB fraction drastically improves material's bulk properties [7,8]. This result clearly demonstrates that the effect of grain boundary character distribution on intergranular corrosion susceptibility is not a linear one. It has been pointed out that the beneficial effect of thermomechanical treatment may not necessarily result in a change in the CSLB distribution [9]. By tracking the deviation of grain boundary misorientation from exact matching, lower deviation was observed with annealing time. The term fine tuning was coined to explain the fact that the non-CSLBs might have been slightly improved in terms of properties; and the relative specialness rather than absolute specialness may have resulted without the increase in CSLB distribution [10]. It is suggested here that the geometrical definition of grain boundary structure does not provide a direct correlation with material's bulk properties. The relationship between energetic description and grain boundary geometry is probably needed to have a clearer understanding of the beneficial effect of CSLB on material's bulk properties. Further research is now in progress to substantiate this result.

CONCLUSIONS

Grain boundary character distribution of commercial grade 304 stainless steel can be altered by simple thermomechanical processing. Increasing the CSLB fraction moderately to 54% can drastically reduce the susceptibility to intergranular corrosion of 304 stainless steels. It is envisioned that this simple thermomechanical processing may be adapted for commercial purpose to produce a new grade of 304 stainless steel with high CSLB fraction significantly improving its intergranular corrosion susceptibility.

ACKNOWLEDGMENTS

The authors gratefully acknowledge the facilities provided by the Nuclear Engineering Material Laboratory, and the Scientific and Technological Research Equipment Center, Chulalongkorn University. This work was supported by the **Thailand Research Fund** under grant number RSA/02/2540.

REFERENCES

- 1. V. Thaveeprungsriporn, A. Junyuyen, and W. Ratanachai, J. of Electron Microscopy Society fo Thailand, vol.11, no.1, (1997), pp. 24.
- 2. A.J. Schwartz and W.E. King, JOM, February, 1998, pp. 50.
- 3. G.S. Was, V. Thaveeprungsriporn, and D.C. Crawford, JOM, February, 1998, pp. 44.
- 4. G. Palumbo, International Patent Application no. PCT/CA93/00556.
- 5. P. Lin, G. Palumbo, and K.T. Aust, Scripta Materialia, 36, 10, (1997), pp. 1145.
- 6. G. Palumbo and K.T. Aust, in Recrystallization 90, T.Chandra ed., TMS-AIME, (1990), pp.101.

- 7. V. Thaveeprungsriporn and G.S. Was, <u>Metallurgical and Materials Transactions A</u>, 28A., (1997), pp. 2101.
- 8. D.C. Crawford and G.S. Was, Metallurgical Transactions A, 23A, (1992), pp. 1195.
- 9. C.B. Thomson and V. Randle, Acta Materialia, 45, (1997), pp. 4909.
- 10. V. Randle, Acta Materialia, 47, 15, (1999), pp. 4187.

Table 1 Summary of the effect of iterative strain annealing on grain size and CSLB distribution.

Specimen	Initial grain size (µm)	Initial percent CSLB	Strain annealing step	Grain size (µm)	Percent CSLB
A	- 1100		1	25	26
(recrystallized at	14	36	2	29	41
800°C/30 min)	-		3	31	45
В			1	31	44
(recrystallized at	24	34	2	32	28
850°C/2hr)			3	30	54
С	1		1	28	39
(recrystallized at	31	41	2	31	39
950°C/4hr)	1		3	28	46

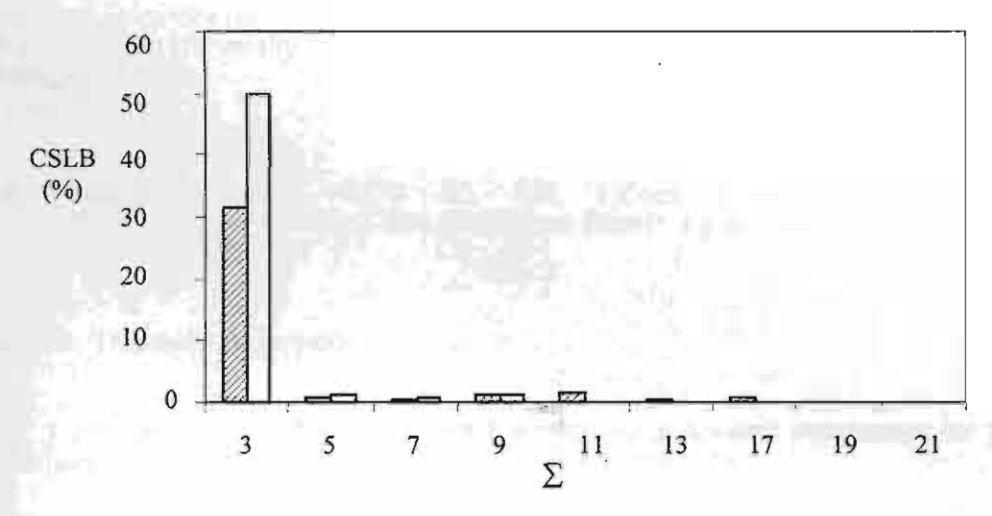


Figure 1 Comparison of the grain boundary character distribution of specimens with different CSLB fraction.

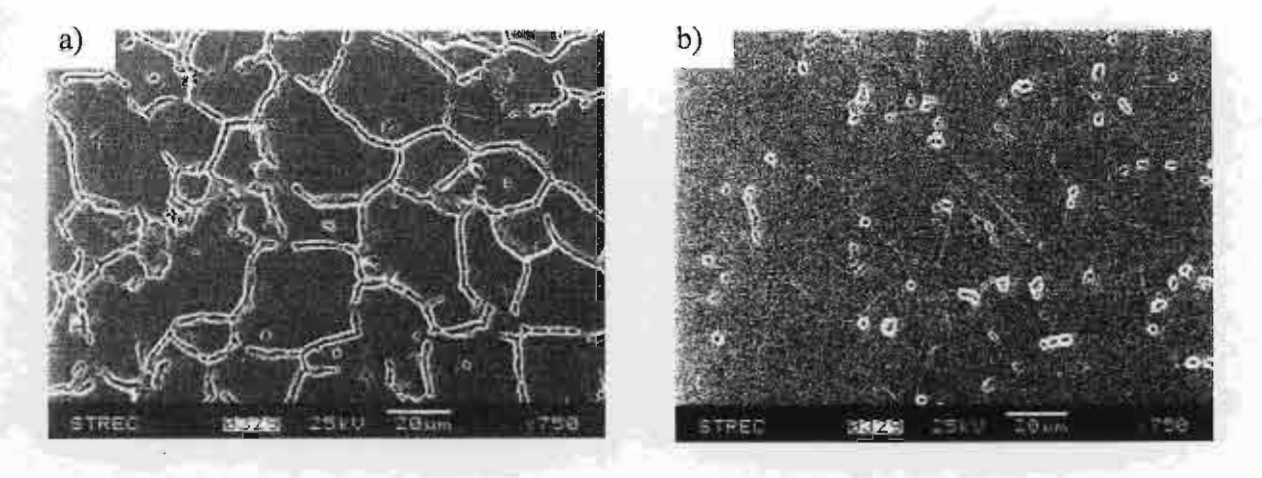


Figure 2 The effect of CSLB fraction on intergranular corrosion of specimens with (a) 36% CSLB fraction and (b) 54% CSLB fraction.

MATERIALIA

Professor Subra Suresh, Co-ordinating Editor Professor Richard Wagner, Co-ordinating Editor

Principal Editors:

Dr. Ladislas P. Kubin (Mechanical and Functional Properties) Professor Hirotaro Mori (Structural and Functional Characterization) Professor Andreas Mortensen (Processing, Synthesis and Phase Transformations) Professor Ramamoorthy Ramesh (Physical and Functional Properties)

Professor Andreas Mortensen

École Polytechnique Fédérale de Lausanne Département des Matériaux Laboratoire de Métallurgie Méchanique MX-D Ecublens CH - 1015 Lausanne

Switzerland Tel: +41 (0)21 693 2912 Fax: +41 (0)21 693 4664

E-mail: Scripta@eptl.ch

Lausanne, August 11, 2000

Dr. Visit Thaveeprungsriporn Dept. of Nuclear Technology Fyculty of Engineering Chulalongkorn University Nbangkok 10330 Thailand

Ref: Manuscript No.S - 0179 - 00 - AM, "Effect of Iterative Strain Annealing on Grain Boundary Network of 304 Stainless Steel" by V. Thaveeprungsriporn, P. Sinsrok and D. Thong-Aram

Dear Dr. Thaveeprungsriporn,

I am pleased to inform you that I accept your revised manuscript for publication to Scripta Materialia, and that I am sending this manuscript to the printer.

Sincerely.

Prof. Andreas Mortensen

EFFECT OF ITERATIVE STRAIN ANNEALING ON GRAIN BOUNDARY NETWORK OF 304 STAINLESS STEEL

V. Thaveeprungsriporn, P. Sinsrok, and D. Thong-Aram Department of Nuclear Technology, Faculty of Engineering, Chulalongkorn University, Bangkok, Thailand 10330

Keywords: Strain Annealing; Grain Boundary; Triple Junction; EBSD; Austenite Steel

Introduction

Interest in controlling grain boundary structure to achieve the desirable bulk properties in polycrystals has resulted in a search to find the processing parameters to enhance the frequency of structurally ordered low- Σ coincidence-site-lattice boundaries (CSLBs). The optimization of the CSLBs is usually performed through thermomechanical processes which rely on combinations of strain and annealing. Approaches by iterative strain annealing and recrystallization have been shown to be an effective and commercially practical method of increasing the CSLB fraction while retaining small grain sizes (1,2). Although the CSLB classification has been found to correlate well with several properties, it is still considered to be an insufficient criterion for specialness since its designation does not directly specify the crystallography at the boundary plane itself. However, there have been relatively few investigations which addresses this parameter due to technical complexities associated with grain boundary plane measurement (3).

It is also well known that the specific free energies of grain boundaries meeting at a triple junction can be compared by measuring the equilibrium dihedral angles to the three grain boundaries (4,5). The dihedral angle is related to the grain boundary energy by the expression (6):

$$\gamma_a / \sin \alpha = \gamma_b / \sin \beta = \gamma_c / \sin \delta,$$
 [1]

where γ_a , γ_b , and γ_c are the grain boundary energies joined at a triple junction, and α , β , and δ are the respective interfacial angles. Hence, the dihedral angle can be used as a measure of the grain boundary energy (7). An effort is already underway to extract grain boundary energies from triple junction geometry in polycrystalline MgO (8).

The objective of this study is to demonstrate that the geometrical data on the dihedral angle distribution can be used to characterize the grain boundary network complementing the crystallographic data as described by the CSLB distribution. Iterative strain annealing was employed to alter the grain boundary character distribution of commercial grade 304 stainless steel, the CSLB and dihedral angle distributions were quantifiably described and compared following each strain annealing treatment.

Experimental

As-received 304 stainless steel rods (Fe-18.49Cr-9.21Ni-1.07Mn-0.036C) were first sectioned into pieces of 2 inches long, and then solutionized at 1050° C for 2 hr. Specimens were then forged 30%, and recrystallized at 800° C for 0.5 hr, 850° C for 2 hr, and 950° C for 4 hr to produce different grain sizes. Specimens further received 3% in compression and annealed at 950° C for 10 min. A total of 3 sequential strain-annealing steps were employed. The orientations of grains were characterized using automated electron back-scattering diffraction system (OPAL-Oxford Instrument) in a JEOL 5800LV scanning electron microscope. The CSLB classification was based on Brandon's criterion (9) and only Σ values up to 29 are considered. Dihedral angles were measured directly from scanning electron micrographs taken at a minimum magnification of 750x. For each sample, at least 200 grains were crystallographically characterized and more than 70 triple junctions (210 grain boundaries) were quantified for their dihedral angles. It should be noted that triple junctions containing coherent twin boundaries were excluded from the dihedral angle measurement.

Results and Discussion

Table 1 summarizes the effect of iterative strain annealing on grain sizes and CSLB distribution. Following the first strain-annealing step, the thermomechanical treatment had resulted in some grain growth in specimens recrystallized at 800° C/0.5hr and 850°C/2hr. However, almost no change in mean grain size was observed following the 2^{nd} and 3^{rd} strain annealing steps. The entire thermomechanical processes did not affect the mean grain size of specimens that were initially recrystallized at 950°C/4hr. Although there is no clear systematic pattern of how the CSLB distribution altered with each strain-annealing step, the third heat-treating step resulted in an overall increase in the CSLB fraction reaching the maximum of 57%. Further, nearly all of the CSLB fractions are Σ 3 boundaries and no statistical significant of twin related boundaries (Σ 9 and Σ 27) were observed.

Lin et al. (10) showed that at high $\Sigma 3$ densities (>40%), geometric contributions strongly influence the final $\Sigma 3^n$ distribution. The twin-limited microstructure (TLM) model first proposed by Palumbo et al. (11) suggests that the maximum theoretical limit of 67% $\Sigma 3$ should likely result in 100% CSL distribution. The absence of twin-related boundaries, $\Sigma 9$ and $\Sigma 27$, even with a $\Sigma 3$ fraction up to 50% did not support the TLM model. The $\Sigma 3$ regeneration model recently proposed by Randle (12) is more applicable to explain how the iterative strain annealing process only enhance the $\Sigma 3$ boundary fraction observed in this study. The model shows how interface interactions in a twinned material generate $\Sigma 3$ boundaries without promoting the $\Sigma 3^n$ boundaries. Further, the strain annealing treatments had resulted in very little change in mean grain size, and thus, the $\Sigma 3$ regeneration model which is based on the mobility and dislocation absorption mechanism rather than the Fullman-Fisher twin formation model via grain growth is more relevant.

A moderate increase in the CSLB distribution does not translate directly into an expected moderate improvement in properties. It has been shown that only a moderate increase in the CSLB fraction in high purity nickel-base alloy via iterative strain annealing can improve creep and cracking properties remarkably (13). It was proposed that the significant improvement on the observed creep behavior is associated with different grain boundary types conjoined at a triple junction. It is not

an individual specialness of each CSLB that is important, but rather how it is distributed and influenced the entire grain boundary network connected through the triple junctions. Since the dihedral angle is related to the grain boundary network through surfaces connected along triple junctions, the measurement of dihedral angle distribution was adopted to explore a link between the CSLB distribution and its influence on the grain boundary network. Figure 1 summarizes the distribution of dihedral angles following each thermomechanical treatment. It can be seen that the distributions are very distinctive with some showing sharper distribution around 120° than others. It is also worth noting that despite very little change in the mean grain size there are substantial differences in dihedral angle distributions indicating significant grain boundary activities during each strain annealing step.

To statistically describe the dihedral angle distribution, the standard deviation (S.D.) which signifies the shape of the distribution was calculated and plotted with the CSLB distribution, Figure 2. It is clear that a fairly good linear correlation between the CSLB fraction and the standard deviation of the grain boundary dihedral angle distribution was observed. Higher CSLB fraction specimens possess a flatter distribution of dihedral angles while sharper distribution around 120° is observed in specimens with lower CSLB fraction. From eq.[1], if all three boundaries meeting at a triple junction are of equal in energies, a uniform 120° distribution is expected. Hence, various dihedral angle distributions of thermomechanically treated specimens indicate different proportions of energies presence in the system. In an attempt to quantifiably describe the dihedral angle distribution, the cumulative frequency of dihedral angles (CFDA) around the mean value of 120° was investigated. The CFDA parameter is introduced as a first approximation to describe grain boundary fraction within specific group of angles, and thus energies. Figure 3 shows the plot of the CFDA between 120°+/-10° and 120°+/-20° and grain boundary type fraction. It is interesting to see that the CFDA between 120°+/-10° accounts for nearly 40% in lower CSLB fraction. The CFDA monotonically decreases with decreasing high angle boundary (HAB) fraction or increasing CSLB fraction. The specimen with 57% CSLB fraction has a CFDA between 120°+/-10° of only 24%. The most striking result is the observed correlation between the HAB fraction and the CFDA between 120°+/-20°. The CFDA can be translated almost directly into the HAB fraction. This result clearly demonstrates that there is an intimate link between grain boundary type

As such, it is suggested here that the dihedral angle distribution can be used to provide information related to the grain boundary network, and thus the properties of polycrystals. Although it appears that the CSLB distribution is closely related to the dihedral angle distribution, the result may not be generalized. Since most of the CSLBs observed in this study are of $\Sigma 3$ type, these boundaries are likely to include a high proportion of tilt or twist boundary planes, and thus a lower energy configuration (14).

Summary

It has been shown that iterative strain annealing can moderately enhance the CSLB fraction in commercial 304 stainless steel. Investigation of dihedral angles as a mean to confer grain boundary energy and network reveal an intimate link with the grain boundary character distribution. The cumulative frequency dihedral angle (CFDA) parameter was found to correlate well with the misorientation distribution described by the CSLB fraction.

Acknowledgments

The authors gratefully acknowledge the facilities provided by the Nuclear Engineering Material Laboratory, and the Scientific and Technological Research Equipment Center, Chulalongkorn University. The assistance of Ms. Prapapak Sriduang and Mr. Somehai Baotong was also greatly appreciated. This work was supported by the **Thailand Research Fund** under grant number RSA/02/2540.

References

- 1. V. Thaveeprungsriporn and G.S. Was, Metall. and Mat. Trans. 28A, 2101 (1997).
- 2. A.J. Schwartz and W.E. King, JOM, February, 50 (1998).
- 3. V. Randle, Acta Mater. 46, 5, 1459 (1997).
- 4. H. Gleiter and B. Chalmers, Prog. Mater. Sci. 16, 13 (1972).
- 5. L.E. Murr, Interfacial Phenomena in Metals and Alloys, Addison-Wesley, (1975).
- 6. C. Herring, in Physics of Powder Metallurgy, W. Kingston ed., McGraw-Hill, NY, (1951).
- 7. A. Morawiec, Scripta Mater. 41, 1, 13 (1999).
- 8. B.L. Adams, D. Kinderlehrer, W.W. Mullins, A.D. Rollett, and S. Ta'asan, Scripta Mater. 38, 531 (1998).
- 9. D.G. Brandon, Acta Metall. 14, 1479 (1966).
- 10. P. Lin, G. Palumbo, and K.T. Aust, Scripta Mater. 36, 10, 1145 (1997).
- 11. G. Palumbo, K.T. Aust, U. Erb, P.J. King, A.M. Brennenstuhl, and P.C. Lichtenberger, Phys. Stat. Sol. (a) 131, 425 (1992).
- 12. V. Randle, Acta Mater. 47, 15, 4187 (1999).
- 13. G.S. Was, V. Thaveeprungsriporn, and D.C. Crawford, JOM, February, 44 (1998).
- 14. V. Randle, Mater. Sci. Technol. 7, 985 (1991).

Table 1. Summary of the effect of iterative strain annealing on grain size and CSLB population.

Recrystallized	Initial	Initial	Strain Annealed	Mean	CSLB	Σ3
Temperature	Grain Size	CSLB	3% compression	Grain Size	Percent	Percent
and Time	(µm)	Percent	+ 950°C/10min	(µm)		
		36	1 st	25	32	24
800°C/0.5 hr 14	14		2 nd	29	47	35
			3 rd	31	49	40
-			1 st	31	47	41
850°C/2hr	24	34	2 nd	32	33	23
350 572.11			3 rd	30	57	50
			1 st	28	43	36
950°C/4hr	30	38	2 nd	31	42	31
			3 rd	28	47	42

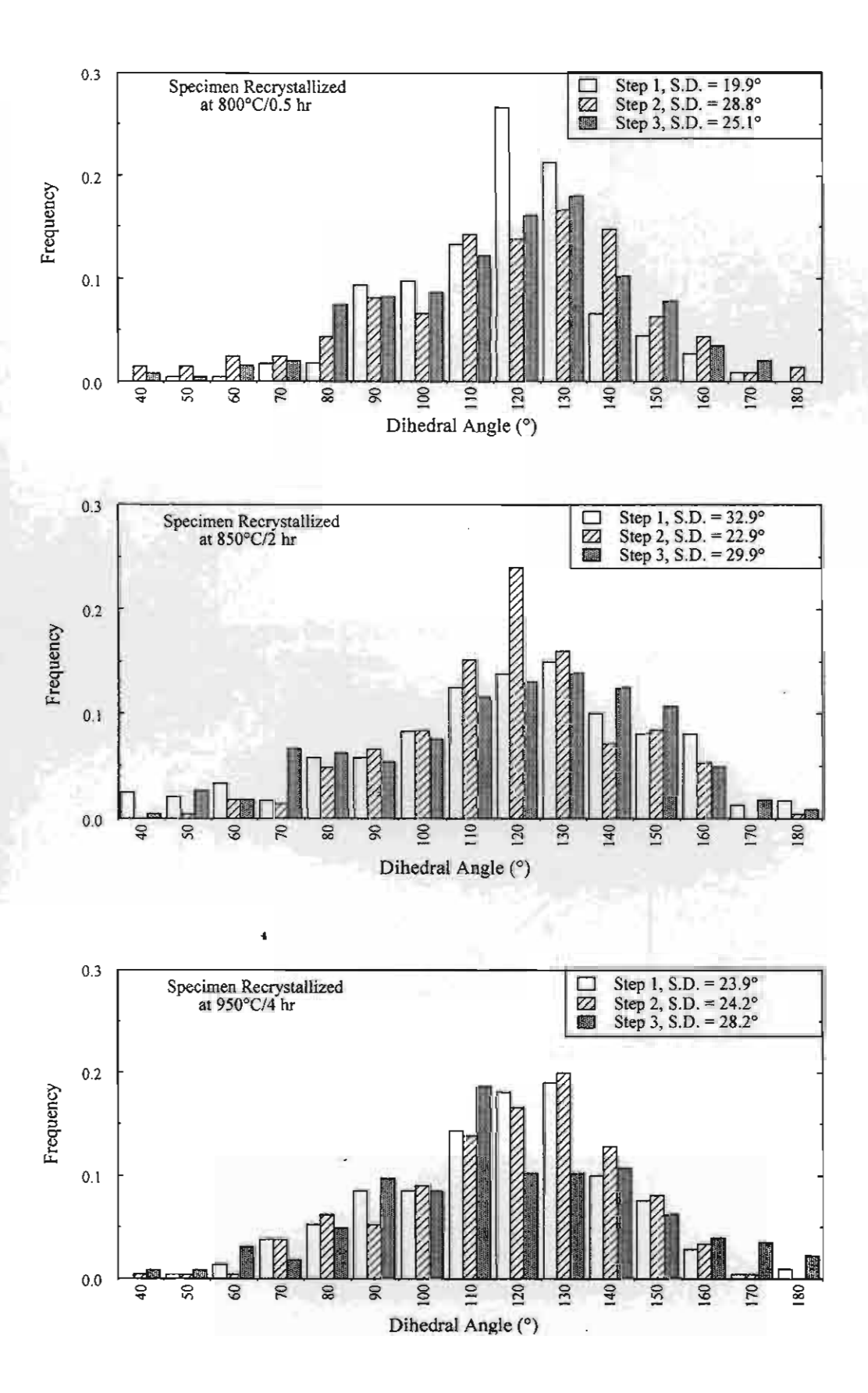


Figure 1. The effect of iterative strain annealing on dihedral angle distribution.

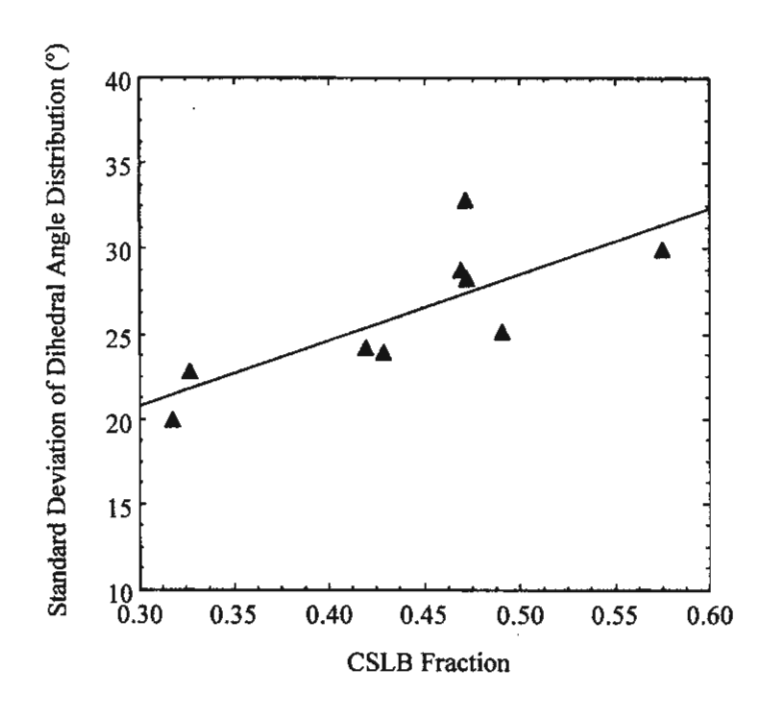


Figure 2. Correlation between the CSLB fraction and the standard deviation of dihedral angle distribution.

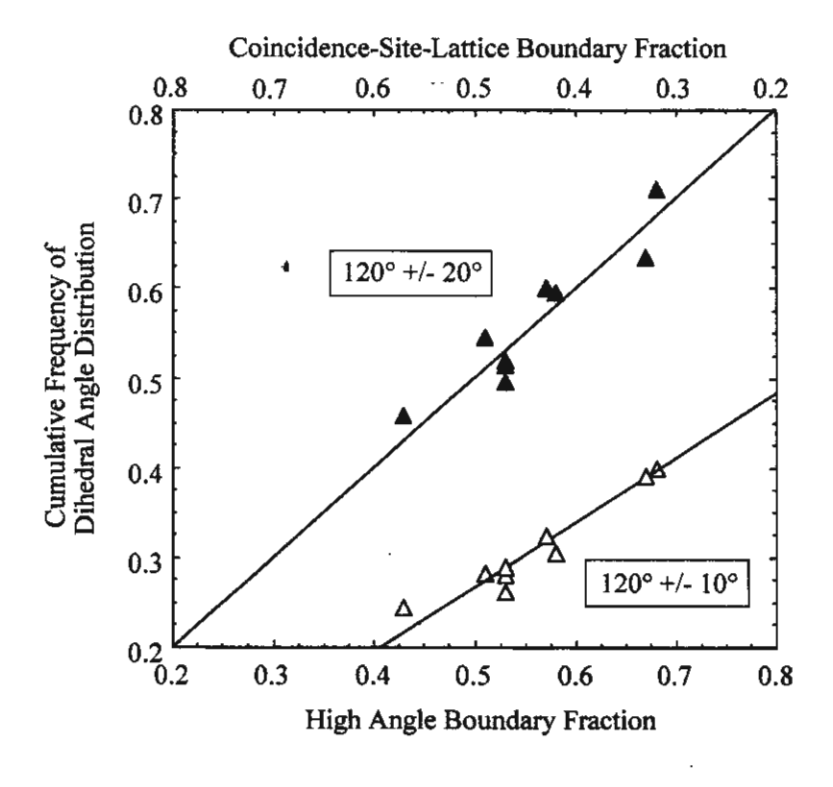


Figure 3. Correlation between the cumulative frequency of dihedral angle distribution and grain boundary character distribution.